

# Temporal dynamics of spectral bioindicators evidence biological and ecological differences among functional types in a cork oak open woodland

Sofia Cerasoli<sup>1</sup> · Filipe Costa e Silva<sup>1</sup> · João M. N. Silva<sup>1</sup>

Received: 2 July 2014 / Revised: 23 September 2015 / Accepted: 27 September 2015 / Published online: 8 October 2015  
© ISB 2015

**Abstract** The application of spectral vegetation indices for the purpose of vegetation monitoring and modeling increased largely in recent years. Nonetheless, the interpretation of biophysical properties of vegetation through their spectral signature is still a challenging task. This is particularly true in Mediterranean oak forest characterized by a high spatial and temporal heterogeneity. In this study, the temporal dynamics of vegetation indices expected to be related with green biomass and photosynthetic efficiency were compared for the canopy of trees, the herbaceous layer, and two shrub species: cistus (*Cistus salvifolius*) and ulex (*Ulex airensis*), coexisting in a cork oak woodland. All indices were calculated from in situ measurements with a FieldSpec3 spectroradiometer (ASD Inc., Boulder, USA). Large differences emerged in the temporal trends and in the correlation between climate and vegetation indices. The relationship between spectral indices and temperature, radiation, and vapor pressure deficit for cork oak was opposite to that observed for the herbaceous layer and cistus. No correlation was observed between rainfall and vegetation indices in cork oak and ulex, but in the herbaceous layer and in the cistus, significant correlations were found. The analysis of spectral vegetation indices with fraction of absorbed PAR (fPAR) and quantum yield of chlorophyll fluorescence ( $\Delta F/F_m$ ) evidenced strongest relationships with the indices Normalized Difference Water Index (NDWI) and Photochemical Reflectance Index (PRI)<sub>512</sub>, respectively. Our results, while confirms the ability of spectral vegetation indices to represent temporal dynamics of biophysical properties of

vegetation, evidence the importance to consider ecosystem composition for a correct ecological interpretation of results when the spatial resolution of observations includes different plant functional types.

**Keywords** Spectral vegetation indexes · In situ spectral measurements · Vegetation heterogeneity · Cork oak open woodlands · Mediterranean forest

## Introduction

In recent years, the use of remote sensing products to retrieve biophysical properties of vegetation encountered growing interest for ecology studies. Spectral vegetation indices (VIs) are increasingly applied to monitor physiological and phenological changes of canopies and frequently integrated into productivity models (Yuan et al. 2014; Cheng et al. 2014). A frequent application are gross primary productivity (GPP) estimates following a data-model fusion approach theoretically based on the light use efficiency (LUE) concept (Monteith 1972, 1977). The LUE equation presumes a linear relationship between GPP and the photosynthetic active radiation absorbed by vegetation (absorbed photosynthetic active radiation (APAR)), where LUE is the slope of the regression line. The attractiveness of this approach relies on the possibility of obtaining all input parameters from remote sensing data (Ollinger 2010) enhancing the reliability of estimates based on structural and climate parameters (Carvalho et al. 2010). APAR is the result of the incident photosynthetic active radiation (PAR) multiplied by the fraction of absorbed PAR (fPAR) which is generally assumed to be linearly related with the Normalized Difference Vegetation Index (NDVI) (Myneni and Williams 1994; Sims et al. 2006). LUE is parameterized according to the vegetation type (Running et al. 2004) and

✉ Sofia Cerasoli  
sofiac@isa.ulisboa.pt

<sup>1</sup> Centro de Estudos Florestais, Instituto Superior de Agronomia, Universidade de Lisboa, Lisboa, Portugal

environmental constraints (Carvalhais et al. 2010; Potter et al. 1993) or estimated by the Photochemical Reflectance Index (PRI) (Drolet et al. 2008).

Despite the general assumption of the linear relationship between fPAR and NDVI, in some cases, other indices showed better performance than NDVI. Under low vegetation cover, for example, the Enhanced Vegetation Index (EVI) (Gao et al. 2000) and the Modified Soil-Adjusted Vegetation Index (MSAVI) (Rondeaux et al. 1996) demonstrated to be able to correct for the interference of soil reflectance. On the opposite, in dense vegetation, it was observed that NDVI saturates and the fPAR-NDVI relationship is not linear (Brantley et al. 2011; Huete et al. 2002). In grasslands subjected to water and nutrient stress, Cristiano et al. (2010) compared the performance of different indices and identified a modified NDVI, named green NDVI (GNDVI) as the best estimator for grasslands fPAR. Other authors suggest the use of chlorophyll indices (CI) to improve fPAR estimates (Sims et al. 2006). The Normalized Difference Water Index (NDWI), initially developed to estimate tissue water content (Gao 1996), was also found useful to estimate leaf biomass and hence also fPAR, in crops from semiarid environments (Bolton and Friedl 2013) and the leaf area index in boreal forests (Heiskanen et al. 2013). It appears evident that a VI maintaining a consistent relationship with fPAR independently of vegetation structure is still lacking.

The ability of PRI to represent LUE dynamics depends mainly on plant functional types. In herbaceous species, GPP seasonality is expected to depend essentially on greenness and fPAR while limited changes in LUE (and PRI) are expected (Gamon et al. 1995; Tagesson et al. 2012). On the opposite, in evergreen tree species, only small changes are expected to occur in NDVI across time while PRI is expected to reflect changes in LUE and assumes primary importance for GPP determination (Sims et al. 2006; Gamon et al. 1995). In semideciduous shrubs, an intermediate behavior is expected, but large differences were observed among species in the LUE-PRI relationship (Filella et al. 2004).

The time step of measurements is also important for interpreting LUE dynamics. On a daily basis, experimental evidences show that the PRI-LUE relationship depends on transient changes in the ratio of pigments of the xanthophylls cycle and the instantaneous efficiency of photosystem II (Penuelas et al. 1995). At longer time steps, from weeks to seasons, PRI variability is also strongly influenced by changes in chlorophylls and carotenoid pigments resulting by changes in canopy structure and phenology (Soudani et al. 2014; Gamon and Bond 2013; Barton and North 2001) and possibly leading to a misinterpretation of PRI trends. Therefore, several alternative PRI formulations have been tested to reduce these interferences (Hernandez-Clemente et al. 2011; Porcar-Castell et al. 2012). Nonetheless, the number of field studies testing different alternatives for PRI is still limited.

An additional source of variability in the relationship between VIs and the biological properties of vegetation, relevant for forest and agroforestry systems, is the coexistence and frequent spatial overlap of different plant functional types. Mediterranean open oak woodlands are particularly challenging in this context. These agroforestry systems are characterized by a discontinuous tree canopy and an understory characterized by an herbaceous layer interposed by shrubs (Bugalho et al. 2011). As a result, oak woodlands present a mosaic of vegetation highly dynamic in time and space.

Previous studies on similar ecosystems demonstrated that VI information obtained from remote sensing was useful to estimate productivity (Chiesi et al. 2005; Garbulsky et al. 2008; Maselli et al. 2009; Ogutu and Dash 2013), but these studies, performed at the ecosystem level without distinguishing among functional types, do not contribute to the understanding of the relationship between VIs and biophysical properties of vegetation and results cannot be explained from an ecophysiological point of view. The collection of VIs retrieved by in situ spectral measurements of coexisting plant functional types (PFTs) permits to compare seasonal dynamics of biological properties of vegetation. This is a prerequisite to the application of VIs in ecology studies and fundamental to a correct interpretation of remote sensing retrievals at the ecosystem scale.

Time series of VIs make also possible to study inter- and intra-seasonal response patterns of vegetation to climate parameters, which are useful for predictive studies, of major relevance in the actual climate change context (Schimel et al. 2015). The Mediterranean region is expected to be particularly vulnerable to changes in climate patterns (Giorgi and Lionello 2008). An analysis of the VIs-climate relationship can be useful to understand how biophysical variables are influenced by climate drivers and at which time step for each PFT.

The main goal of this study is to assess differences in the VIs representing fPAR and LUE among different PFTs coexisting in a cork oak woodland. Specifically, we intend to answer to the following questions: (1) Are the temporal patterns of NDVI and PRI different among PFTs? Large differences are expected between evergreen oaks and the seasonal herbaceous layer, but the response of shrubs is difficult to predict. (2) Are other indices better estimators of fPAR and LUE than NDVI and PRI, respectively, for the PFTs included in this study? (3) Does the relationship between climate drivers and VIs diverge among PFTs?

## Methods

### Study site

Field measurements were collected in a 50-year-old cork oak woodland (*Quercus suber* L.) located in central Portugal (39°

08° 20.9' N, 9° 19' 57.7" W, 165-m altitude). Climate is typically Mediterranean with hot and dry summer while more than 80 % of the annual precipitation is concentrated between October and April. The average annual precipitation recorded at the climate station of Santarém (39° 12' N, 8° 44' W) for the period 1981–2010 was 652 mm, and mean daily temperature was 17 °C ([www.ipma.pt/pt/oclima/normais.clima](http://www.ipma.pt/pt/oclima/normais.clima)). The soil is a cambisol (FAO), with 81 % sand, 5 % clay, and 14 % silt. Tree density is 177 tree ha<sup>-1</sup> and leaf area index (LAI) is 1.5. The mean height below the canopy and total height of trees are 3.1 and 7.9 m, respectively. The mean diameter at breast height is 24.7 cm (Correia et al. 2013). The understory is composed of a mixture of shrubs and herbaceous species. A survey of the understory composition performed in June 2013, following the pin-point method (Kent and Coker 1992), showed that shrubs and herbaceous species represented 27.6 and 39.2 %, respectively, of the understory layer cover fraction, while the remaining is covered by litter and bare soil. *Cistus salvifolius* (cistus) and *Ulex airensis* (ulex) are the most represented shrub species and have contrasting growth habit and drought resistance. The ulex has shoots and leaves modified into spines and deep roots conferring high drought resistance. The cistus has shallow roots and a semideciduous habit, losing part of its foliage during the summer drought to limit transpiration (Correia et al. 2013; Werner et al. 1999). The herbaceous layer is dominated by grasses (44.5 %) and legumes (28.7 %).

Measurements were performed on cork oak trees, cistus, and ulex individuals. Herbaceous plots were delimited by 50 × 50-cm quadrats. Cork oak leaves shedding period was estimated by the leaf biomass collected every 10 days from baskets randomly positioned below the tree canopy. Nadir view photographs of each target (tree canopy, shrub, and herbaceous plots) were taken at each measurement day for qualitative assessment of phenology. Rainfall (ARG100, Environmental Measurements Ltd., Gateshead, UK), solar radiation (BF2, Delta-T Devices Ltd., Cambridge, UK), humidity, and air temperature (CS215, Campbell Scientific, Inc., Logan, UT, US) are collected continuously and averaged at a 30-min time step (CR10X, Campbell Scientific) at the top of a 22-m-tall tower located in the site, as part of an eddy covariance system, measuring carbon and water fluxes at the scale of the ecosystem (Costa-e-Silva et al. 2015).

### Spectral measurements

The observations were acquired with a FieldSpec3 spectroradiometer (ASD Inc., Boulder, USA), which provided hyperspectral reflectance data in the range of 350–2500 nm, from April 2011 to October 2013, on a monthly basis. The visible and near-infrared region (350–1000 nm) is measured with a spectral resolution (full-width half maximum) of 3 nm and a sampling interval of 1.4 nm. The mid infrared region

(1000–2500 nm) is measured with a spectral resolution of 10 nm and a sampling interval of 2.0 nm. Spectra were collected from the canopy of six cork oak trees, four cistus and four ulex shrubs, and four herbaceous quadrats. The targets were selected within the study area among those fully exposed to sun radiation. Measurements of tree canopy were done using a scaffold on the south side of the canopy. All measurements were performed with a nadir view, a field of view angle of 25°, and a distance of about 90 cm from the target, covering an area with a diameter of approximately 40 cm. All measurements were conducted within 2 h around solar noon, to minimize the effects of shadowing and solar zenith changes, with five replicates of each target, each representing the average of 25 spectra, with the bare fiber optic cable inserted into a pistol grip. A white reference of known reflectance (Spectralon panel, Labsphere, Inc., North Sutton, USA) was used to normalize for variations in atmospheric conditions and to convert the measurements into absolute reflectance.

### fPAR measurements

The fraction of PAR intercepted by the canopy (fPAR) was measured using a linear PAR ceptometer (AccuPar LP-80 Decagon Devices Inc., Pullman, WA, USA) for the same trees, shrubs, and herbaceous plots where spectral measurements were conducted. The radiation intercepted by the canopy was considered approximately equal to absorbed radiation, as the amount of reflected radiation in the PAR range is usually small (Gower et al. 1999). Measurements of incident (PAR<sub>i</sub>) and transmitted PAR (PAR<sub>t</sub>) were used to compute fPAR according to the following equation:

$$fPAR = \frac{1 - PAR_t}{PAR_i}$$

For each target, at least two measurements above the canopy and three (herbaceous plots), five (shrubs), or eight (trees) measurements below the canopy were taken. All measurements were performed on the same day of spectral measurements, also around solar noon. Measurements were interrupted between November and February, when the fraction of incident to total PAR radiation was less than 0.8 due to the low solar zenith angle.

### Chlorophyll fluorescence

Chlorophyll fluorescence measurements were performed only for cork oak leaves because the configuration of the fluorimeter leaf clip did not permit to perform measurements of the herbaceous layer or shrubs. Three sunlit terminal shoots were collected from the upper south-facing side of the tree canopy, where canopy spectral measurements were performed. Measurements of chlorophyll fluorescence and reflectance were

immediately performed on six fully expanded leaves per tree. The maximum ( $Fm'$ ) and current fluorescence ( $F$ ) were measured at natural day light conditions using the pulse-modulated fluorimeter Mini-PAM (Heinz Walz, Effeltrich, Germany). The quantum yield, an estimator of the photosynthetic efficiency of photosystem II, was calculated as follows:  $\Delta F/Fm'$ , where  $\Delta F = Fm' - F$  (Genty et al. 1989).

## Data analysis

Measurements of canopy reflectance were used to build up spectral VIs. Narrow band indices were selected from the literature among those known of potential interest as green biomass or photosynthetic LUE estimators (Table 1). Pearson correlation coefficient was applied to analyze the strength of the relationship between VIs and meteorological variables averaged at different time windows: 0, 5, 10, 30, and 90 days back since the day of data collection. After a first screening of the data, the 0- and 10-day time windows were discarded from the analysis, as results were never consistently different from those at 5-day time window. The meteorological variables analyzed were as follows: daytime average PAR (PAR,  $\mu\text{mol m}^{-2} \text{s}^{-1}$ ), air temperature (Temp, °C), vapor pressure deficit (VPD, hPA), and total rainfall (mm).

Pearson coefficient was also applied to determine the degree of correlation ( $r$ ) between the spectral VIs and biophysical properties of vegetation (fPAR and  $\Delta F/Fm'$ ). Linear regressions were established for the pairs of variables showing strongest correlations for each PFT, and slopes of regressions were tested for differences among PFTs by comparing their confidence intervals. Conditions of normal distribution and homoscedasticity were always verified. Statistics were performed by the use of the IBM SPSS Statistics package (v20).

## Results

### Conditions during the experiment

During the experimental period, from April 2011 to October 2013, seasonal patterns of temperature and PAR were similar (Fig. 1). The maximum and the minimum daily average temperatures were always recorded in August and in January, respectively. The two hydrological years (October–September) of 2011–2012 and 2012–2013 were different from the normal average (1960–1990) of 650 mm, being 35 % lower in 2011–2012 (418 mm) and 20 % higher in 2012–2013 (798 mm). In the dry year of 2011–2012, rainfall was concentrated in the periods of October–November and April–May, while in 2012–2013, rainfall was distributed between October and March.

### Temporal patterns of NDVI and PRI

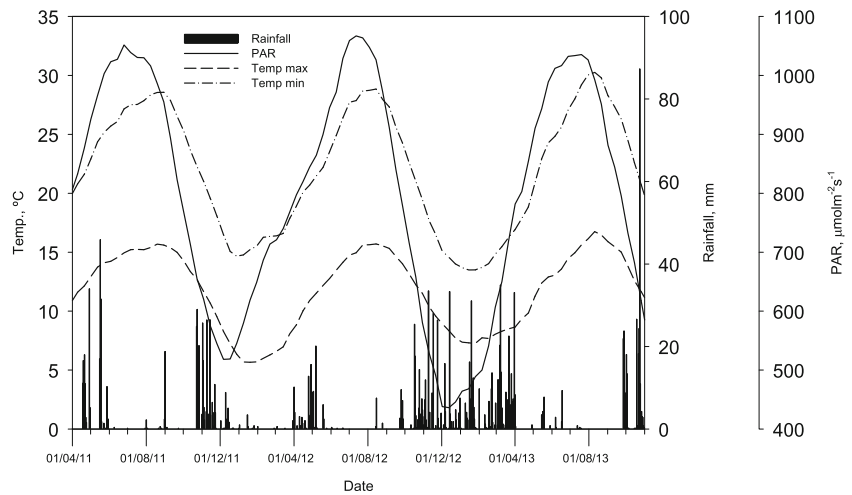
Marked differences were observed in the NDVI temporal trends among the oak canopy (Fig. 2a), the herbaceous layer (Fig. 2b), and the shrub species (Fig. 2c). Cork oak canopy showed small changes across time, ranging from 0.7 to 0.85. Nonetheless, a constant decrease was observed from July 2011 to May 2012 and again from July 2012 to April 2013. The trend is clearly related with leaf ontogeny, and the lowest peak observed corresponded to the period of most intense leaf yellowing and shedding that occurs yearly in cork oak. The herbaceous layer, on the contrary, showed the largest NDVI range, shifting from 0.2 to 0.7, with the lowest values observed during the senescence and drying out that extended from May to October in 2011 and 2013 and anticipated to March in the dry year of 2012. The atypical low precipitation

**Table 1** Spectral indices tested in this study

Name	Formula	References	
Green biomass			
NDVI	Normalized Difference Vegetation Index	$(R_{800} - R_{670}) / (R_{800} + R_{670})$	Rouse et al. (1974)
GNDVI	Normalized Difference Vegetation Index green	$(R_{750} - R_{550}) / (R_{750} + R_{550})$	Gitelson and Merzlyak (1998)
EVI	Enhanced Vegetation Index	$2.5 * (R_{NIR} - R_{Red}) / (R_{NIR} + 6 * R_{Red} - 7.5 * R_{Blue} + 1)$	Gao et al. (2000)
MSAVI	Modified Soil-Adjusted Vegetation Index	$[(R_{800} - R_{670})(1 + L)] / (R_{800} + R_{670} + L)$	Qi et al. (1994)
CI	Chlorophyll index	$(R_{750} - R_{705}) / (R_{750} + R_{705})$	Gitelson and Merzlyak (1994)
NDWI	Normalized Difference Water Index	$(R_{860} - R_{1240}) / (R_{860} + R_{1240})$	Gao (1996)
Photosynthetic light use efficiency			
PRI	Photochemical Reflectance Index	$(R_{570} - R_{531}) / (R_{570} + R_{531})$	Gamon et al. (1992)
PRI <sub>512</sub>		$(R_{512} - R_{531}) / (R_{512} + R_{531})$	Hernandez-Clemente et al. (2011)
PRI <sub>545</sub>		$(R_{570} - R_{545}) / (R_{570} + R_{545})$	Gamon et al. (1997); Porcar-Castell et al. (2012)

Indices were divided into two groups: indices correlated with green biomass and indices correlated with photosynthetic light use efficiency. Coefficients applied for EVI are those adopted by the MODIS-EVI algorithm

**Fig. 1** Ten-day moving average of average daily maximum (dashed line), minimum temperature (dash-dotted line), and PAR (solid line). Total daily rainfall is represented by vertical bars. Data shown have been recorded on the site between April 2011 and October 2013



recorded between October 2011 and June 2012 affected also the amount of green biomass of the herbaceous layer as evident from the differences in the maximum NDVI recorded. In the hydrological year 2011–2012, the maximum value of NDVI (0.53) was observed in December, while in the following growing season, NDVI reached 0.71 in March, suggesting that the growth of the herbaceous layer lasted for a longer period in the wet year (see Figs. 1 and 2b). The two shrub species (Fig. 2c) showed different seasonal patterns. The semideciduous cistus showed a marked decrease of NDVI during summer months, and the minimum annual value was recorded every year at the end of the summer, before the return of autumn rains. The ulex showed a much smaller drop of NDVI during summer, as compared to cistus. For ulex in both years of 2012 and 2013, it was possible to appreciate a

decrease of NDVI in February and March related with the appearance of yellow flowers.

The range of PRI values was smaller than the observed for NDVI; however, it was still possible to appreciate seasonal patterns. In 2011–2012 and 2012–2013, the PRI value increased in cork oak from December to April and then decreased sharply (Fig. 2d). The highest observed values of PRI corresponded to the lowest NDVI values (Fig. 2a), when old yellow leaves prevail in the canopy. The lowest values were observed after old leaves shed, when the canopy is exclusively composed of new leaves, and corresponded to the highest values of NDVI observed. Between June and December, PRI was low and constant around 0.05. The herbaceous layer showed a smaller variation in PRI than the other functional types, ranging from 0.05 to 0.1 (Fig. 2e) with no evident

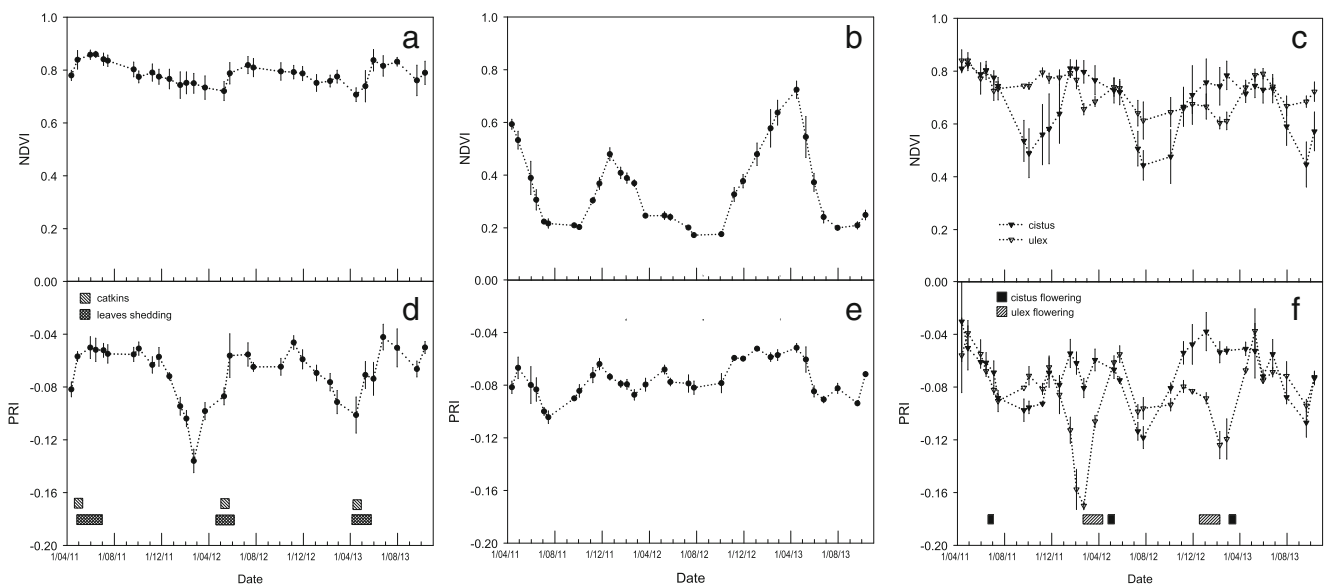


**Fig. 2** Average values of NDVI and PRI measured in cork oak (a, d), herbaceous layer (b, e), and shrubs (c, f) in a Mediterranean oak woodland from April 2011 to October 2013. Each point represents the average of six replicates for trees, six to eight for shrubs, and four for the

herbaceous layer. Vertical bars represent standard errors of the mean. At the bottom are reported phenological events: catkin development (left-hatched bars) and leaf shedding (crossed bars) of cork oak, flowering of cistus (closed bars), and ulex (right-hatched bars)

seasonal pattern. In both shrub species, cistus, and ulex (Fig. 2f), an increasing trend was observed from April/June to August/September. Similar to the observed for cork oak, also for ulex, maximum PRI values were recorded in March, which corresponded to the lower NDVI.

### fPAR and spectral indices

We tested different green biomass VIs for their correlation with fPAR (Table 2). NDWI showed the highest correlation coefficient ( $r$ ) for the oak canopy, herbaceous layer, and cistus. NDVI also showed significant correlations with fPAR, but less strong than the observed for NDWI, especially for the herbaceous layer. In this PFT, GNDVI also showed a significant correlation to fPAR. The CI, generally assumed to be representative of chlorophyll content, showed a significant correlation with fPAR for the herbaceous layer and the cistus. The last showed the higher degree of correlation for any of the tested indices. On the contrary, no significant correlation was found for ulex for any index. A linear regression analysis (Table 6) was performed for NDWI in oak canopy (Fig. 3a), the herbaceous layer (Fig. 3b), and cistus (Fig. 3c) to assess its potential as estimator of fPAR. The comparison of slopes showed no differences in the regression line among PFTs.

### Chlorophyll fluorescence and spectral indices

The spectral indices expected to be related with photosynthetic efficiency, PRI, PRI<sub>512</sub>, and PRI<sub>545</sub> (see Table 1) were tested for their correlation with  $\Delta F/Fm'$ . At both leaf and canopy levels, PRI<sub>512</sub> showed a better performance than the other indices ( $r=0.647^{**}$ , against 0.334 and 0.422, respectively, for PRI and PRI<sub>545</sub>). A significant linear relationship was verified only for PRI<sub>512</sub> and  $\Delta F/Fm'$  (Fig. 4) ( $\Delta F/Fm'=0.825 \cdot \text{PRI}_{512} + 0.317$ ,  $r=0.635$ ,  $P<0.0001$ ).

**Table 2** Pearson correlation coefficient ( $r$ ) between selected vegetation indexes and fPAR measurements in different species and vegetation types in a cork oak woodland ( $N=31$  for oak canopy,  $N=24$  for herbaceous layer,  $N=49$  for cistus,  $N=47$  for ulex)

Vegetation index	$R$			
	Oak canopy	Herbs	Cistus	Ulex
NDVI	0.564**	0.424*	0.771**	-0.178
GNDVI	0.298	0.470*	0.658**	-0.253
EVI	0.241	0.356	0.623**	-0.159
MSAVI	0.257	0.350	0.633**	-0.144
CI	0.282	0.454*	0.725**	-0.113
NDWI	0.599**	0.573**	0.833**	-0.092

\*Correlations significant at the 95 %; \*\*correlations significant at 99 %

### The influence of climate variables

Correlations between VIs and climate drivers (temperature, PAR, rainfall, and VPD) were analyzed for each PFT and within the shrub PFT for the two species, at time windows of 5, 30, and 90 days (Tables 3, 4, 5, and 6). Generally, contrasting patterns were observed between VIs related with green biomass (NDVI, GNDVI, EVI, MSAVI, CI, NDWI) and those representing photosynthetic efficiency (PRI, PRI<sub>512</sub>, and PRI<sub>545</sub>). Correlations were different for cork oak, herbaceous layer, and shrub species and depended also on the time window. In oak canopies (Table 3), positive correlations were observed between Temp, PAR, and VPD and the indices NDVI, GNDVI, CI, and NDWI, while correlations were negative for PRI and similar indices. Correlations with rainfall were always weak and not significant. The strongest correlations with Temp, PAR, and VPD were observed for the NDWI on a 30-day time window. On the same time window, PRI<sub>512</sub> showed globally the highest correlations with PAR, VPD, and Temp, but on a 90-day time window, correlations with the same variables were stronger for PRI and PRI<sub>545</sub> than PRI<sub>512</sub>.

The correlations for the herbaceous layer showed marked differences from what was observed for cork oak (Table 4). For almost all pairs of variables, correlation coefficient increased as the time window increased, showing their maximum at 90-day time window. At this time window, NDVI showed the best correlations with Temp, rainfall, PAR, and VPD. Among the VIs related with photosynthetic performance, the PRI<sub>512</sub> on a 90-day time window showed highest correlations with climate drivers.

The semideciduous shrub cistus, similarly to the observed for the herbaceous layer, showed that VIs represent better the influence of climate drivers on biological properties of vegetation on a 90-day time window (Table 5). At this time window, GNDVI was the index best correlated with Temp and PAR, while CI showed the highest correlations with rainfall and VPD. Similar increase of correlation coefficient with longer time windows, but opposite trend with the meteorological variables, was observed for estimators of photosynthetic LUE, with PRI and PRI<sub>545</sub> showing similar performance and, in both cases, better than the observed for PRI<sub>512</sub>. The ulex showed generally weak correlations between VIs and meteorological variables (Table 6). Only rainfall showed a positive, significant correlation with VIs related with green biomass (NDVI, GNDVI, and CI). Similar to the observed for the herbaceous layer and the cistus, better correlations were obtained on a 90-day time window. Correlations with rainfall were significant for CI and, in a lesser extent, for NDVI and GNDVI. PRI<sub>512</sub> showed better performance than PRI and PRI<sub>545</sub> and positive significant correlations with Temp and VPD on a 90-day time window.

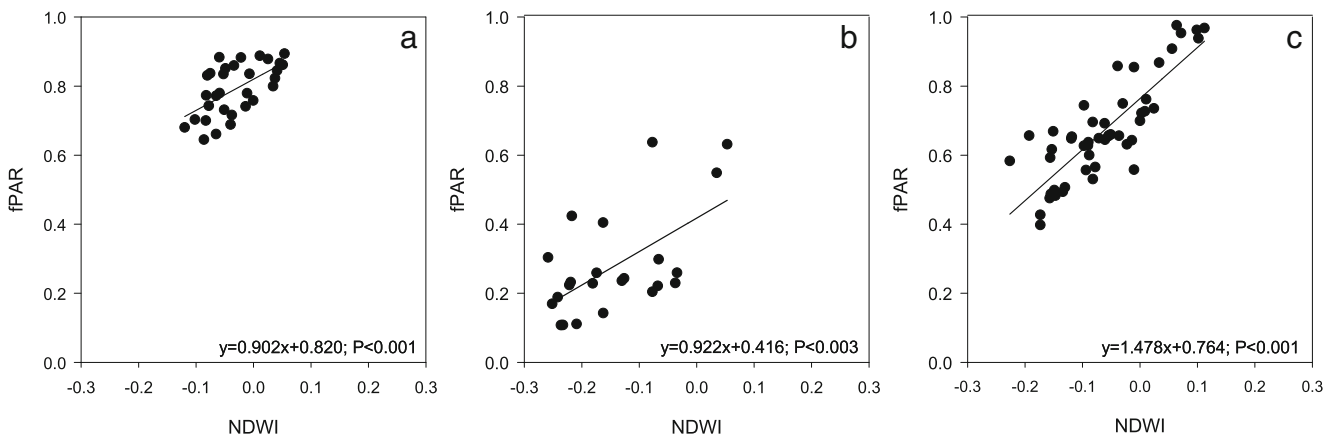


**Fig. 3** Relationships observed “in situ” between fPAR and NDWI, for cork oak canopy (a), herbaceous layer (b), and cistus (c). Regression line parameters are shown in the *bottom* of the figure

## Discussion

### NDVI and PRI temporal trends

Our results show clear differences among functional groups in the temporal trends of NDVI and PRI. NDVI was fairly stable along the experimental period, for the cork oak, in contrast to the seasonal marked pattern observed in the herbaceous layer, with the only exception of a decrease observed every year in correspondence with the peak of leaf fall. This effect was also observed in holm oak (Soudani et al. 2014) and confirms the ability of VIs to mirror seasonal dynamics also in evergreen species with small temporal changes in canopy structure. On the other way, shrubs showed differences in their NDVI trend among the

two species, particularly during the summer period, when the semideciduous cistus reduces considerably its foliage and a drop in NDVI was observed. Similarly, studies in ecosystems dominated by shrub species reported a decrease in NDVI during summer stress (Fuentes et al. 2006), and comparative studies of deep-rooted and shallow-rooted shrub species showed a decrease of NDVI in the second with the onset of summer drought (Piñol et al. 1998), underlining the ability of this VI to represent differences in the response of shrubs to stress conditions.

In contrast with the NDVI trends, larger amplitude of values was observed for PRI in the cork oak canopy than in the herbaceous layer, and differently from what observed for the herbaceous layer, both cork oak canopy and shrubs showed marked seasonal PRI trends. This VI proved to be related to LUE in a considerable number of experiments (Garbulsky et al. 2011), and seasonal trends have been observed in long-term studies in evergreen species such as holm oak (Soudani et al. 2014) or conifers (Cheng et al. 2009), while in shrubs, results are contrasting and depend on the species (Filella et al. 2004). In the present study, the seasonal trends observed in cork oak and shrub species were different, which was also evidenced by the differences observed in the correlation sign between PRI and climate variables, suggesting a different physiological response of trees and shrubs to climate drivers. While our results clearly show that temporal patterns of NDVI and PRI were able to track differences in the seasonal trend of different functional groups, they also evidence drawbacks in the ecological interpretation of VIs. For example, PRI peaks were observed in shrubs in correspondence of flowering, due to the distinctive spectral signature of the flowers, as observed also in other shrub communities (Filella et al. 2004) and alert for the need to associate spectral information with phenological data, for example, photographs, which allow to date the flowering (Fig. 2). Most important, differences in temporal trends observed among vegetation types alert for the importance of the knowledge about species composition and their spatial arrangement in the interpretation of VIs retrieved in heterogeneous forests from remote platforms.

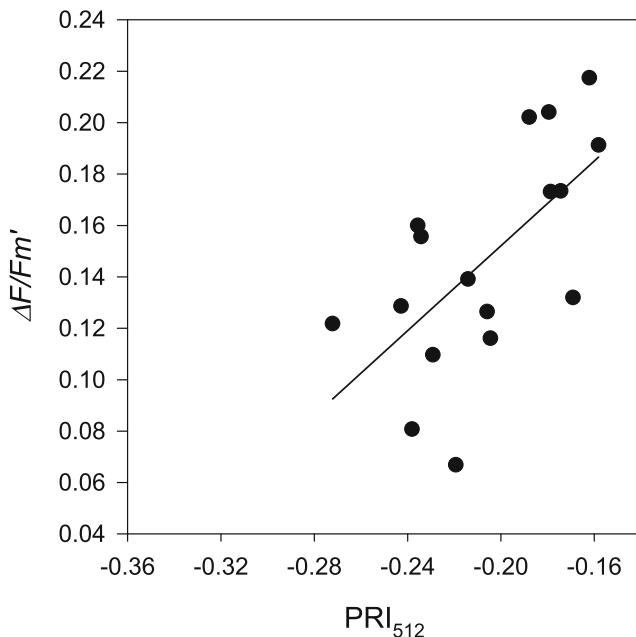


**Fig. 4** Relationships observed between leaf  $\Delta F/Fm'$  and  $PRI_{512}$  obtained from canopy cork oak spectral measurements. Each *point* is the average of five replicates per six tree ( $N=30$ ) measurements on the same day

**Table 3** Correlation coefficients between VIs and climate variables for cork oak

	NDVI	GNDVI	EVI	MSAVI	CI	NDWI	PRI	PRI <sub>512</sub>	PRI <sub>545</sub>
5-day time									
PAR ( $\mu\text{mol m}^{-2} \text{s}^{-1}$ )	0.52**	0.40*	-0.53**	-0.54**	0.31	0.68***	-0.25	-0.73***	-0.36*
Temp ( $^{\circ}\text{C}$ )	0.46**	0.40*	-0.27	-0.28	0.43*	0.60***	-0.59***	-0.63***	-0.54**
VPD (hPa)	0.26	0.29	-0.26	-0.27	0.31	0.40*	-0.38*	-0.35*	-0.32
Rainfall (mm)	-0.12	-0.12	0.17	0.18	-0.03	-0.25	-0.08	0.18	-0.32
30-day time									
PAR ( $\mu\text{mol m}^{-2} \text{s}^{-1}$ )	0.61***	0.52**	-0.34*	-0.35*	0.45**	0.79***	-0.41*	-0.78***	-0.49***
Temp ( $^{\circ}\text{C}$ )	0.60***	0.56***	0.02	0.01	0.61***	0.67***	-0.71***	-0.62***	-0.69***
VPD (hPa)	0.47**	0.47**	-0.04	-0.04	0.46**	0.60**	-0.47**	-0.53**	-0.46**
Rainfall (mm)	-0.03	0.10	0.12	0.12	-0.02	-0.16	-0.12	0.10	-0.09
90-day time									
PAR ( $\mu\text{mol m}^{-2} \text{s}^{-1}$ )	0.58***	0.58***	-0.01	-0.02	0.63***	0.68***	-0.68***	-0.60***	-0.69***
Temp ( $^{\circ}\text{C}$ )	0.44*	0.52**	0.39*	0.39*	0.65***	0.43*	-0.74***	-0.27	-0.69***
VPD (hPa)	0.33	0.42*	0.26	0.26	0.52**	0.36*	-0.62***	-0.25	-0.57***
Rainfall (mm)	0.09	-0.07	0.00	0.00	-0.08	0.03	0.05	-0.14	0.04

Climate variables are represented as the average (PAR, Temp, and VPD) or the sum (rainfall) of values over 5-, 30-, or 90-day time windows back since the collection of spectral measurements in the field. Best correlation for pair of variables is highlighted in italics

\*Correlations significant at the 95 %; \*\*correlations significant at 99 %; \*\*\*correlations significant at 99.9 %

### Other VI representatives of fPAR and photosynthetic efficiency

Despite the good agreement observed among all indices of the group of VIs related with green biomass, NDWI showed highest correlations with fPAR than any other index for oak canopies, herbaceous layer, and cistus, and we suggest the

possibility of applying this index for fPAR estimations in different functional types. The NDWI has been originally developed to estimate water content of vegetation (Gao 1996), but it has been already shown that it is also a good predictor of leaf biomass in crops from semiarid regions (Bolton and Friedl 2013) and LAI in boreal forest (Heiskanen et al. 2013). Similar to the reported by Heiskanen et al. (2013), we observed

**Table 4** Correlation coefficients between VIs and climate variables for the herbaceous layer

	NDVI	GNDVI	EVI	MSAVI	CI	NDWI	PRI	PRI <sub>512</sub>	PRI <sub>545</sub>
5-day time									
PAR ( $\mu\text{mol m}^{-2} \text{s}^{-1}$ )	-0.35*	-0.10	-0.20	-0.15	-0.29	-0.03	0.55***	0.35*	0.50**
Temp ( $^{\circ}\text{C}$ )	-0.54**	-0.34*	-0.45**	-0.40*	-0.46**	-0.29	0.53**	0.50**	0.57**
VPD (hPa)	-0.48**	-0.27	-0.43*	-0.37*	-0.42*	-0.31	0.60***	0.45**	0.57***
Rainfall (mm)	0.09	-0.08	-0.02	-0.05	0.07	-0.04	-0.41*	-0.08	-0.27
30-day time									
PAR ( $\mu\text{mol m}^{-2} \text{s}^{-1}$ )	-0.52**	-0.24	-0.31	-0.25	-0.45**	-0.16	0.65***	0.52**	0.68***
Temp ( $^{\circ}\text{C}$ )	-0.65***	-0.48**	-0.53**	-0.47**	-0.59***	-0.43*	0.54**	0.62***	0.65***
VPD (hPa)	-0.67***	-0.44*	-0.53**	-0.47**	-0.61***	-0.46**	0.67***	0.65***	0.75***
Rainfall (mm)	0.40*	0.16	0.24	0.21	0.39*	0.27	-0.64***	-0.42*	-0.60***
90-day time									
PAR ( $\mu\text{mol m}^{-2} \text{s}^{-1}$ )	-0.77***	-0.58***	-0.62***	-0.56***	-0.71***	-0.52**	0.64***	0.75***	0.77***
Temp ( $^{\circ}\text{C}$ )	-0.69***	-0.63***	-0.62***	-0.58***	-0.66***	-0.62***	0.42*	0.64***	0.56***
VPD (hPa)	-0.74***	-0.67***	-0.71***	-0.68***	-0.71***	-0.70***	0.47**	0.70***	0.63***
Rainfall (mm)	0.77***	0.71***	0.74***	0.69***	0.74***	0.79***	-0.49**	-0.74***	-0.63***

Climate variables are represented as the average (PAR, Temp, and VPD) or the sum (rainfall) of values over 5-, 30-, or 90-day time windows back since the collection of spectral measurements in the field. Best correlation for pair of variables is highlighted in italics

\*Correlations significant at the 95 %; \*\*correlations significant at 99 %; \*\*\*correlations significant at 99.9 %



**Table 5** Correlation coefficients between VIs and climate variables for cistus

	NDVI	GNDVI	EVI	MSAVI	CI	NDWI	PRI	PRI <sub>512</sub>	PRI <sub>545</sub>
5-day time									
PAR ( $\mu\text{mol m}^{-2} \text{s}^{-1}$ )	-0.03	-0.37*	0.15	0.14	-0.25	0.27	0.31	-0.27	0.15
Temp ( $^{\circ}\text{C}$ )	-0.40*	-0.71***	-0.30	-0.31	-0.58***	-0.19	0.44*	0.07	0.40*
VPD (hPa)	-0.33	-0.55***	-0.16	-0.15	-0.47**	-0.13	0.37*	0.11	0.33
Rainfall (mm)	0.02	0.10	-0.21	-0.24	0.09	-0.15	-0.16	0.04	-0.08
30-day time									
PAR ( $\mu\text{mol m}^{-2} \text{s}^{-1}$ )	-0.18	-0.49**	0.01	0.00	-0.42*	0.12	0.48**	-0.18	0.30
Temp ( $^{\circ}\text{C}$ )	-0.58***	-0.81***	-0.47***	-0.47***	-0.73***	-0.39*	0.60***	0.20	0.56***
VPD (hPa)	-0.56***	-0.73***	-0.38*	-0.36*	-0.72***	-0.34	0.68***	0.23	0.61***
Rainfall (mm)	0.09	0.07	-0.11	-0.12	0.19	-0.06	-0.40*	-0.04	-0.25
90-day time									
PAR ( $\mu\text{mol m}^{-2} \text{s}^{-1}$ )	-0.59***	-0.80***	-0.47**	-0.47**	-0.74***	-0.39*	0.66***	0.20	0.57***
Temp ( $^{\circ}\text{C}$ )	-0.76***	-0.81***	-0.73***	-0.72***	-0.79***	-0.72***	0.62***	0.47**	0.64***
VPD (hPa)	-0.78***	-0.80***	-0.75***	-0.74***	-0.83***	-0.73***	0.66***	0.50**	0.71***
Rainfall (mm)	0.55***	0.41*	0.47**	0.45**	0.55***	0.51**	-0.62***	-0.47**	-0.62***

Climate variables are represented as the average (PAR, Temp, and VPD) or the sum (rainfall) of values over 5-, 30-, or 90-day time windows back since the collection of spectral measurements in the field. Best correlation for pair of variables is highlighted in italics

\*Correlations significant at the 95 %; \*\*correlations significant at 99 %; \*\*\*correlations significant at 99.9 %

similar parameters for the NDWI-fPAR regression line for oak trees and shrubs, strongly suggesting the use of this index for fPAR estimates in heterogeneous ecosystems. This index could be particularly interesting in the perspective of the use of spectral retrievals at a low spatial resolution where different PFTs are undistinguished, to describe green biomass temporal trends at the ecosystem level.

Similarly to previous studies (Cristiano et al. 2010), in the herbaceous layer, the GNDVI showed higher correlations with fPAR than NDVI. The two shrub species revealed a contrasting pattern, with the ulex showing no correlations between fPAR and VIs and the cistus showing highly significant correlation degrees with all VIs. Obviously, this is the result of different growth habit and physiognomy. While the

**Table 6** Correlation coefficients between VIs and climate variables for ulex

	NDVI	GNDVI	EVI	MSAVI	CI	NDWI	PRI	PRI <sub>512</sub>	PRI <sub>545</sub>
5-day time									
PAR ( $\mu\text{mol m}^{-2} \text{s}^{-1}$ )	0.11	-0.08	-0.11	-0.12	0.05	0.30	-0.34	-0.06	-0.28
Temp ( $^{\circ}\text{C}$ )	0.11	-0.08	-0.05	-0.05	0.00	0.09	-0.55**	0.16	-0.39*
VPD (hPa)	0.06	-0.14	0.00	0.00	-0.04	0.11	-0.26	0.01	-0.17
Rainfall (mm)	0.01	0.05	0.00	0.00	0.04	-0.11	-0.10	0.08	-0.11
30-day time									
PAR ( $\mu\text{mol m}^{-2} \text{s}^{-1}$ )	0.08	-0.14	-0.02	-0.02	-0.04	0.24	-0.36*	0.05	-0.26
Temp ( $^{\circ}\text{C}$ )	0.04	-0.10	-0.01	-0.01	-0.10	-0.02	-0.47**	0.30	-0.29
VPD (hPa)	-0.01	-0.17	0.00	0.02	-0.17	0.05	-0.24	0.13	-0.12
Rainfall (mm)	0.15	0.23	0.04	0.03	0.26	-0.03	-0.30	0.05	-0.32
90-day time									
PAR ( $\mu\text{mol m}^{-2} \text{s}^{-1}$ )	-0.03	-0.16	-0.07	-0.07	-0.18	-0.06	-0.38*	0.34	-0.18
Temp ( $^{\circ}\text{C}$ )	-0.06	-0.09	0.02	0.02	-0.21	-0.26	-0.29	0.45***	-0.09
VPD (hPa)	-0.06	-0.08	-0.05	-0.05	-0.21	-0.24	-0.26	0.39*	-0.05
Rainfall (mm)	0.37*	0.35*	0.31	0.30	0.49**	0.33	-0.29	-0.17	-0.44**

Climate variables are represented as the average (PAR, Temp, and VPD) or the sum (rainfall) of values over 5-, 30-, or 90-day time windows back since the collection of spectral measurements in the field. Best correlation for pair of variables is highlighted in italics

\*Correlations significant at the 95 %; \*\*correlations significant at 99 %; \*\*\*correlations significant at 99.9 %

semideciduous cistus is subjected to temporal changes in its leaf area, as showed also by the NDVI temporal trend, in the ulex, due to its peculiar modified leaves and the green bark that covers most of the branches, the absence of a relationship between VIs and LAI (and fPAR) was expected. Contrary to the observed in other studies on low-density vegetation (Ma et al. 2014), the EVI did not produce better results than NDVI in its correlations with fPAR. EVI is expected to reduce the effect of soil background reflectivity (Huete et al. 2002) which was likely to influence the spectral signature of the canopy in the present study, subjected to seasonal drought and canopy cover decrease. Nonetheless, similar results have been previously observed in similar ecosystem (Cheng et al. 2006), where EVI increased the noise of the temporal trend, as compared to NDVI.

Our results showed that, for cork oak, PRI<sub>512</sub> is a better estimator of photosynthetic efficiency than PRI. Previous studies showed significant correlations between the quantum yield and PRI, not found in this study. Gamon et al. (1997) found a consistent positive linear relationship between PRI and quantum yield across different functional types. The PRI-quantum yield relationship was also found significant under superimposed drought conditions in tree species on a short term (Ripullone et al. 2011); however, other studies reported a weak PRI-quantum yield correlations, especially under long-term experimental conditions (Hmimina et al. 2014). The PRI<sub>512</sub> index was previously adopted by Hernandez-Clemente et al. (2011) in *Pinus* species (*Pinus nigra* and *Pinus sylvestris*) and demonstrated to reduce the variability caused by changes in the structure of the canopy. The study of Hernandez-Clemente et al. (2011) was performed during summer stress conditions, while our experiment spans across seasons, suggesting that the index is less sensitive than PRI to leaf ontogeny, canopy structure, and background, also subjected to changes along the experiment. Correlations observed between PRI<sub>512</sub> and climate drivers confirm our results on the suitability of this spectral index for photosynthetic efficiency monitoring. In another study, Porcar-Castell et al. (2012) reported a better performance of PRI<sub>545</sub> than PRI as estimator of photosynthetic efficiency across seasons in Scots pine. In our study, PRI<sub>545</sub> did not show a better performance in comparison with other indices. The reasons for such different results could be multiple and clearly evidence a need for further long-term studies on the relationship between physiological processes associated with photosynthesis and PRI in the different functional groups.

### The influence of climate drivers on spectral signature

The analysis of the correlations between VIs and climate drivers clearly evidences differences in the biophysical response of different PFTs. The herbaceous layer showed significant and positive correlation between VI estimators of

green biomass and rainfall but negative correlations with Temp, PAR, or VPD, while, for the last three variables, an opposite trend was observed for cork oak. Differences in the timing of annual cycle can explain the contrasting relationships observed. The germination of the herbaceous species occurs in the autumn, after the first rains, and biomass growth is confined to the period February–May (Jongen et al. 2013), strongly depending on precipitation, as indicated by NDVI and rainfall time series (Figs. 1 and 2). At the end of spring, when temperature and VPD raise, the herbaceous biomass is already drying out. In the evergreen cork oak, the annual renewal of the canopy lasts for about 2 months and new leaves are completely developed only at the end of June (see Fig. 2). The existence of a positive relationship between shoot elongation and average temperature (30 days) before budburst was confirmed by phenological studies on the same species in the region (Pinto et al. 2011).

It is noteworthy that the two shrub species showed contrasting patterns in their relationship between VIs and climate drivers; while the ulex showed weak correlations with all climate variables, the cistus showed patterns similar to the herbaceous layer. In this semideciduous shrub species, the reduction of leaf area is an effective strategy to limit water losses by transpiration during the summer months (Harley et al. 1987), which corroborates the positive correlation of VI estimators of biomass and rainfall and the negative correlation of the same VIs with VPD and temperature (Table 5). Globally, our results evidence that phenological differences among PFT are reflected in VIs and suggest caution in the adoption of spectral information in ecology studies from remote platforms without identification of the composition of the vegetation in the study area.

A good agreement has been also observed between VIs related with photosynthetic efficiency (PRI, PRI<sub>512</sub>, and PRI<sub>545</sub>) and climate variables. Also, in this case, the patterns observed were opposite for the cork oak and for the herbaceous layer and the cistus. Globally, these indices were negatively correlated with Temp, PAR, and VPD in cork oak and positively in the herbaceous layer. Again, these differences should be ascribed to differences in the physiological response of different functional types to climate drivers. The herbaceous layer and the shrub cistus showed a strong dependence of VIs on rainfall at a 90-day time window, not observed in cork oak and ulex. In the Mediterranean region, precipitation is the main constrain to photosynthesis and growth (Pereira et al. 2006; Pereira and Chaves 1993) and an exacerbation of water deficit conditions is predicted for the region by climate change scenarios (Giorgi and Lionello 2008). This is particularly critical for shallow-rooted species, like those of the herbaceous layer and the cistus, which are unable to access to groundwater, and justifies the strong correlation observed between VIs and rainfall on a long-term basis. It is less critical for the deeply rooted species such as cork oak (David et al. 2013) or ulex.

Biophysical properties mirrored by VIs showed to be more influenced by climate on a monthly (30-day time window) and seasonal (90-day time window) basis than on a short term (5-day time window). This was true either for VIs related with fPAR as well as with those related with photosynthetic light use efficiency and for all the vegetation types analyzed. In agreement with quantum yield measurements, PRI<sub>512</sub> showed to be the best correlated with climate drivers for cork oak canopy in the short term. When the time window increases, the degree of correlation with PRI and PRI<sub>545</sub> increases and prevails at a 90-day time window. Differences observed in the short and long terms are known to depend on the higher sensitivity of PRI, as compared to PRI<sub>512</sub>, to canopy structure and pigment concentration (Filella et al. 2009; Penuelas et al. 1995; Garbulsky et al. 2011). This can explain the difference observed in the performance of the indices between short and long terms but does not explain the weaker correlation observed for the cistus for PRI<sub>512</sub>, and it is indicative of the need for further studies of the dynamics of photosynthesis and spectral signature in shrub species.

## Conclusions

Results from this study evidence the potential of VIs for monitoring biological properties of vegetation and mirroring the phenological and physiological response of different functional groups to climate drivers. Spectral sensors, as showed in many studies, can be employed as tools in ecology studies and forest management, allowing indirect monitoring of vegetation and increasing the reliability of GPP models. Moreover, in the actual climate change context, with unexpected changes in the seasonal patterns of temperature and precipitation for the Mediterranean area (Giorgi and Lionello 2008), temporal series of VIs make possible to study inter- and intra-seasonal response patterns to climate parameters, which are fundamental for predictive studies (Schimel et al. 2015).

At the same time, the present study suggests that particular care should be taken in the interpretation of spectral information retrieved from remote platforms or in situ observations from the top of tree canopies (Hilker et al. 2011) in heterogeneous ecosystems such as Mediterranean open woodlands. Our results clearly show how differences among PFT seasonal dynamics are represented by VIs. Accounting for those differences is critical to a correct interpretation of the relationship between the spectral signature of the vegetation and its biophysical properties and essential to a correct upscaling of GPP by models integrating optical information (Porcar-Castell et al. 2015).

Results evidence also the need for further studies relating biological and optical properties in different functional groups at different time windows to clarify differences observed between climate drivers and VIs at different time

steps. These studies would contribute to the identification of functional types based on traits distinguishable by optical properties (Ustin and Gamon 2010; Gamon 2015), strengthening the relationship between ecological information and remote sensing observations.

Comparative studies of in situ and remote sensing data are also envisaged to distinguish biological variability from other confounding factors, such as atmospheric conditions, illumination, and observation angles, which are relevant sources of variability when spectral information is retrieved from remote platforms.

**Acknowledgments** Sofia Cerasoli and Filipe Silva are postdoc fellows of the Portuguese *Fundação para a Ciência e Tecnologia, Ministry of Science and education* (BPD/SFRH/78998/2011). João Silva is a research associate at the School of Agriculture, with funding from the FCT (Ciência 2008 program). Field work was funded by FCT (PEst-OE/AGR/UI0239/2011) in the framework of the research activities of the Forest Research Centre.

## References

- Barton CVM, North PRJ (2001) Remote sensing of canopy light use efficiency using the photochemical reflectance index—model and sensitivity analysis. *Remote Sens Environ* 78(3):264–273. doi:10.1016/S0034-4257(01)00224-3
- Bolton DK, Friedl MA (2013) Forecasting crop yield using remotely sensed vegetation indices and crop phenology metrics. *Agr Forest Meteorol* 173:74–84. doi:10.1016/j.agrformet.2013.01.007
- Brantley ST, Zinnert JC, Young DR (2011) Application of hyperspectral vegetation indices to detect variations in high leaf area index temperate shrub thicket canopies. *Remote Sens Environ* 115(2):514–523. doi:10.1016/j.rse.2010.09.020
- Bugalho MN, Caldeira MC, Pereira JS, Aronson JA, Pausas J (2011) Mediterranean oak savannas require human use to sustain biodiversity and ecosystem services. *Front Ecol Environ* 5:278–286
- Carvalhais N, Reichstein M, Collatz GJ, Mahecha MD, Migliavacca M, Neigh CSR, Tomelleri E, Benali AA, Papale D, Seixas J (2010) Deciphering the components of regional net ecosystem fluxes following a bottom-up approach for the Iberian Peninsula. *Biogeosciences* 7(11):3707–3729. doi:10.5194/bg-7-3707-2010
- Cheng Y, Gamon JA, Fuentes DA, Mao Z, Sims DA, H-I Q, Claudio H, Huete A, Rahman AF (2006) A multi-scale analysis of dynamic optical signals in a Southern California chaparral ecosystem: a comparison of field, AVIRIS and MODIS data. *Remote Sens Environ* 103(3):369–378. doi:10.1016/j.rse.2005.06.013
- Cheng Y-B, Middleton EM, Hilker T, Coops NC, Black TA, Krishnan P (2009) Dynamics of spectral bio-indicators and their correlations with light use efficiency using directional observations at a Douglas-fir forest. *Meas Sci Technol* 20(9):095107
- Cheng Y-B, Zhang Q, Lyapustin AI, Wang Y, Middleton EM (2014) Impacts of light use efficiency and fPAR parameterization on gross primary production modeling. *Agr Forest Meteorol* 189–190:187–197. doi:10.1016/j.agrformet.2014.01.006
- Chiesi M, Maselli F, Bindi M, Fibbi L, Cherubini P, Arlotta E, Tirone G, Matteucci G, Seufert G (2005) Modelling carbon budget of Mediterranean forests using ground and remote sensing measurements. *Agr Forest Meteorol* 135(1–4):22–34. doi:10.1016/j.agrformet.2005.09.011

- Correia AC, Costa e Silva F, Correia AV, Hussain MZ, Rodrigues AD, David JS, Pereira JS (2013) Carbon sink strength of a Mediterranean cork oak understorey: how do semi-deciduous and evergreen shrubs face summer drought? *J Veg Sci* 25(2):411–426. doi:10.1111/jvs.12102
- Costa-e-Silva F, Correia AC, Piayda A, Dubbert M, Rebmann C, Cuntz M, Werner C, David JS, Pereira JS (2015) Effects of an extremely dry winter on net ecosystem carbon exchange and tree phenology at a cork oak woodland. *Agric For Meteorol* 204:48–57, doi: **j.agrformet.2015.01.017**
- Cristiano PM, Posse G, Di Bella CM, Jaimes FR (2010) Uncertainties in fPAR estimation of grass canopies under different stress situations and differences in architecture. *Int J Remote Sens* 31(15):4095–4109. doi:10.1080/01431160903229192
- David TS, Pinto CA, Nadezhdina N, Kurz-Besson C, Henriques MO, Quilhó T, Cermak J, Chaves MM, Pereira JS, David JS (2013) Root functioning, tree water use and hydraulic redistribution in *Quercus suber* trees: a modeling approach based on root sap flow. *For Ecol Manage* 307:136–146. doi:10.1016/j.foreco.2013.07.012
- Drolet GG, Middleton EM, Huemmrich KF, Hall FG, Amiro BD, Barr AG, Black TA, McCaughey JH, Margolis HA (2008) Regional mapping of gross light-use efficiency using MODIS spectral indices. *Remote Sens Environ* 112(6):3064–3078. doi:10.1016/j.rse.2008.03.002
- Filella I, Penuelas J, Llorens L, Estiarte M (2004) Reflectance assessment of seasonal and annual changes in biomass and CO<sub>2</sub> uptake of a Mediterranean shrubland submitted to experimental warming and drought. *Remote Sens Environ* 90(3):308–318. doi:10.1016/j.rse.2004.01.010
- Filella I, Porcar-Castell A, Munne-Bosch S, Back J, Garbulsky MF, Penuelas J (2009) PRI assessment of long-term changes in carotenoids/chlorophyll ratio and short-term changes in deoxidation state of the xanthophyll cycle. *Int J Remote Sens* 30(17):4443–4455. doi:10.1080/01431160802575661
- Fuentes DA, Gamon JA, Cheng Y, Claudio HC, H-l Q, Mao Z, Sims DA, Rahman AF, Oechel W, Luo H (2006) Mapping carbon and water vapor fluxes in a chaparral ecosystem using vegetation indices derived from AVIRIS. *Remote Sens Environ* 103(3):312–323
- Gamon JA (2015) Reviews and Syntheses: optical sampling of the flux tower footprint. *Biogeosciences* 12(14):4509–4523. doi:10.5194/bg-12-4509-2015
- Gamon JA, Bond B (2013) Effects of irradiance and photosynthetic downregulation on the photochemical reflectance index in Douglas-fir and ponderosa pine. *Remote Sens Environ* 135:141–149. doi:10.1016/j.rse.2013.03.032
- Gamon JA, Penuelas J, Field CB (1992) A narrow-waveband spectral index that tracks diurnal changes in photosynthetic efficiency. *Remote Sens Environ* 41(1):35–44
- Gamon JA, Field CB, Goulden ML, Griffin KL, Hartley AE, Joel G, Penuelas J, Valentini R (1995) Relationships between NDVI, canopy structure, and photosynthesis in 3 Californian vegetation types. *Ecol Appl* 5(1):28–41
- Gamon JA, Serrano L, Surfus JS (1997) The photochemical reflectance index: an optical indicator of photosynthetic radiation use efficiency across species, functional types, and nutrient levels. *Oecologia* 112(4):492–501. doi:10.1007/s004420050337
- Gao B (1996) NDWI. A normalized difference water index for remote sensing of vegetation liquid water from space. *Remote Sens Environ* 58(3):257–266
- Gao X, Huete AR, Ni WG, Miura T (2000) Optical-biophysical relationships of vegetation spectra without background contamination. *Remote Sens Environ* 74(3):609–620. doi:10.1016/s0034-4257(00)00150-4
- Garbulsky MF, Penuelas J, Papale D, Filella I (2008) Remote estimation of carbon dioxide uptake by a Mediterranean forest. *Glob Change Biol* 14(12):2860–2867. doi:10.1111/j.1365-2486.2008.01684.x
- Garbulsky MF, Penuelas J, Gamon J, Inoue Y, Filella I (2011) The photochemical reflectance index (PRI) and the remote sensing of leaf, canopy and ecosystem radiation use efficiencies: a review and meta-analysis. *Remote Sens Environ* 115(2):281–297. doi:10.1016/j.rse.2010.08.023
- Genty B, Briantais JM, Baker NR (1989) The relationship between the quantum yield of photosynthetic electron-transport and quenching of chlorophyll fluorescence. *Biochimica Et Biophysica Acta* 990(1):87–92
- Giorgi F, Lionello P (2008) Climate change projections for the Mediterranean region. *Global Planetary Change* 2,3:90–104
- Gitelson A, Merzlyak MN (1994) Spectral reflectance changes associated with autumn senescence of *Aesculus Hippocastanum* L and *Acer Platanoides* L. leaves - spectral features and relation to chlorophyll estimation. *J Plant Physiol* 143(3):286–292
- Gitelson AA, Merzlyak MN (1998) Remote sensing of chlorophyll concentration in higher plant leaves. *Adv Space Res* 22(5):689–692. doi:10.1016/S0273-1177(97)01133-2
- Gower ST, Kucharik CJ, Norman JM (1999) Direct and indirect estimation of leaf area index, fAPAR, and net primary production of terrestrial ecosystems. *Remote Sens Environ* 70(1):29–51. doi:10.1016/S0034-4257(99)00056-5
- Harley PC, Tenhunen JD, Beyschlag W, Lange OL (1987) Seasonal changes in net photosynthesis rates and photosynthetic capacity in leaves of *Cistus salvifolius*, a European Mediterranean semi-deciduous shrub. *Oecologia* 74:380–388
- Heiskanen J, Rautiainen M, Stenberg P, Mõttus M, Vesanto V-H (2013) Sensitivity of narrowband vegetation indices to boreal forest LAI, reflectance seasonality and species composition. *ISPRS J Photogramm Remote Sens* 78:1–14. doi:10.1016/j.isprsjprs.2013.01.001
- Hernandez-Clemente R, Navarro-Cerrillo RM, Suarez L, Morales F, Zarco-Tejada PJ (2011) Assessing structural effects on PRI for stress detection in conifer forests. *Remote Sens Environ* 115(9):2360–2375. doi:10.1016/j.rse.2011.04.036
- Hilker T, Gitelson A, Coops NC, Hall FG, Black TA (2011) Tracking plant physiological properties from multi-angular tower-based remote sensing. *Oecologia* 165(4):865–876. doi:10.1007/s00442-010-1901-0
- Hmimina G, Duffrène E, Soudani K (2014) Relationship between photochemical reflectance index and leaf ecophysiological and biochemical parameters under two different water statuses: towards a rapid and efficient correction method using real-time measurements. *Plant Cell Environ* 37(2):473–487. doi:10.1111/pce.12171
- Huete A, Didan K, Miura T, Rodriguez EP, Gao X, Ferreira LG (2002) Overview of the radiometric and biophysical performance of the MODIS vegetation indices. *Remote Sens Environ* 83(1–2):195–213. doi:10.1016/S0034-4257(02)00096-2
- Jongen M, Unger S, Fanguero D, Cerasoli S, Silva JMN, Pereira JS (2013) Resilience of montado understorey to experimental precipitation variability fails under severe natural drought. *Agr Ecosyst Environ* 178:18–30. doi:10.1016/j.agee.2013.06.014
- Kent A, Coker P (1992) *Vegetation description and analysis: a practical approach*. Wiley, New York
- Ma X, Huete A, Yu Q, Restrepo-Coupe N, Beringer J, Hutley LB, Kanniah KD, Cleverly J, Eamus D (2014) Parameterization of an ecosystem light-use-efficiency model for predicting savanna GPP using MODIS EVI. *Remote Sens Environ* 154:253–271. doi:10.1016/j.rse.2014.08.025
- Maselli F, Moriondo M, Chiesi M, Chirici G, Puletti N, Barbati A, Corona P (2009) Evaluating the effects of environmental changes on the gross primary production of Italian forests. *Remote Sens* 1(4):1108–1124. doi:10.3390/rs1041108
- Monteith JL (1972) Solar-radiation and productivity in tropical ecosystems. *J Appl Ecol* 9(3):747–766

- Monteith JL (1977) Climate and efficiency of crop production in Britain. *Philos Trans R Soc Lond Ser B-Biol Sci* 281(980):277–294
- Myneni RB, Williams DL (1994) On the relationship between FAPAR and NDVI. *Remote Sens Environ* 49(3):200–211
- Ogutu BO, Dash J (2013) Assessing the capacity of three production efficiency models in simulating gross carbon uptake across multiple biomes in conterminous USA. *Agr Forest Meteorol* 174:158–169. doi:10.1016/j.agrformet.2013.02.016
- Ollinger SV (2010) Sources of variability in canopy reflectance and the convergent properties of plants. *New Phytol* 189(2):375–394
- Peñuelas J, Filella I, Gamon JA (1995) Assessment of photosynthetic radiation-use efficiency with spectral reflectance. *New Phytol* 131(3):291–296. doi:10.1111/j.1469-8137.1995.tb03064.x
- Pereira JS, Chaves MM (1993) Plant water deficits in Mediterranean ecosystems. In: Smith JAC, Griffiths H (eds) *Water deficits: plant responses from cell to community*. BIOS Scientific, Oxford, pp 237–251
- Pereira JS, Chaves MM, Caldeira MC, Correia AV (2006) Water availability and productivity. In: Morrison JIL, Morecroft D (eds) *Plant growth and climate change*. Blackwell, London, pp 118–145
- Piñol J, Filella I, Ogaya R, Peñuelas J (1998) Ground-based spectroradiometric estimation of live fine fuel moisture of Mediterranean plants. *Agr Forest Meteorol* 90(3):173–186. doi:10.1016/S0168-1923(98)00053-7
- Pinto CA, Henriques MO, Figueiredo JP, David JS, Abreu FG, Pereira JS, Correia I, David TS (2011) Phenology and growth dynamics in Mediterranean evergreen oaks: effects of environmental conditions and water relations. *For Ecol Manage* 262(3):500–508. doi:10.1016/j.foreco.2011.04.018
- Porcar-Castell A, Garcia-Plazaola JI, Nichol CJ, Kolari P, Olascoaga B, Kuusinen N, Fernandez-Marin B, Pulkkinen M, Juurola E, Nikinmaa E (2012) Physiology of the seasonal relationship between the photochemical reflectance index and photosynthetic light use efficiency. *Oecologia* 170(2):313–323. doi:10.1007/s00442-012-2317-9
- Porcar-Castell A, Mac Arthur A, Rossini M, Eklundh L, Pacheco-Labrador J, Anderson K, Balzarolo M, Martín MP, Jin H, Tomelleri E, Cerasoli S, Sakowska K, Hueni A, Julitta T, Nichol CJ, Vescovo L (2015) EUROSPEC: at the interface between remote sensing and ecosystem CO<sub>2</sub> flux measurements in Europe. *Biogeosciences Discuss* 12(15):13069–13121. doi:10.5194/bgd-12-13069-2015
- Potter CS, Randerson JT, Field CB, Matson PA, Vitousek PM, Mooney HA, Klooster SA (1993) Terrestrial ecosystem production: a process model based on global satellite and surface data. *Global Biogeochem Cycles* 7(4):811–841. doi:10.1029/93gb02725
- Qi J, Chehbouni A, Huete AR, Kerr YH, Sorooshian S (1994) A modified soil adjusted vegetation index. *Remote Sens Environ* 48(2):119–126. doi:10.1016/0034-4257(94)90134-1
- Ripullone F, Rivelli AR, Baraldi R, Guarini R, Guerrieri R, Magnani F, Peñuelas J, Raddi S, Borghetti M (2011) Effectiveness of the photochemical reflectance index to track photosynthetic activity over a range of forest tree species and plant water statuses. *Funct Plant Biol* 38(3):177–186. doi:10.1071/FP10078
- Rondeaux G, Steven M, Baret F (1996) Optimization of soil-adjusted vegetation indices. *Remote Sens Environ* 55(2):95–107. doi:10.1016/0034-4257(95)00186-7
- Rouse J, Haas R, Schell J, Deering D (1974) Monitoring vegetation systems in the great plains with ERTS. In: SP-351 N (ed) *Third ERTS Symposium*. NASA, Washington, DC, USA, pp 309–317
- Running SW, Nemani RR, Heinsch FA, Zhao MS, Reeves M, Hashimoto H (2004) A continuous satellite-derived measure of global terrestrial primary production. *Bioscience* 54(6):547–560. doi:10.1641/0006-3568(2004)054[0547:acsmog]2.0.co;2
- Schimel D, Pavlick R, Fisher JB, Asner GP, Saatchi S, Townsend P, Miller C, Frankenberg C, Hibbard K, Cox P (2015) Observing terrestrial ecosystems and the carbon cycle from space. *Glob Change Biol* 21(5):1762–1776. doi:10.1111/gcb.12822
- Sims DA, Luo H, Hastings S, Oechel WC, Rahman AF, Gamon JA (2006) Parallel adjustments in vegetation greenness and ecosystem CO<sub>2</sub> exchange in response to drought in a Southern California chaparral ecosystem. *Remote Sens Environ* 103(3):289–303
- Soudani K, Hmimina G, Dufrene E, Berveiller D, Delpierre N, Ourcival J-M, Rambal S, Joffre R (2014) Relationships between photochemical reflectance index and light-use efficiency in deciduous and evergreen broadleaf forests. *Remote Sens Environ* 144:73–84. doi:10.1016/j.rse.2014.01.017
- Tagesson T, Mastepanov M, Tamstorf MP, Eklundh L, Schubert P, Ekberg A, Sigsgaard C, Christensen TR, Strom L (2012) High-resolution satellite data reveal an increase in peak growing season gross primary production in a high-Arctic wet tundra ecosystem 1992–2008. *Int J Appl Earth Obs Geoinf* 18:407–416. doi:10.1016/j.jag.2012.03.016
- Ustin SL, Gamon JA (2010) Remote sensing of plant functional types. *New Phytol* 186(4):795–816. doi:10.1111/j.1469-8137.2010.03284.x
- Werner C, Correia O, Beyschlag W (1999) Two different strategies of Mediterranean macchia plants to avoid photoinhibitory damage by excessive radiation levels during summer drought. *Acta Oecologica-International Journal of Ecology* 20(1):15–23. doi:10.1016/s1146-609x(99)80011-3
- Yuan W, Cai W, Xia J, Chen J, Liu S, Dong W, Merbold L, Law B, Arain A, Beringer J, Bernhofer C, Black A, Blanken PD, Cescatti A, Chen Y, Francois L, Gianelle D, Janssens IA, Jung M, Kato T, Kiely G, Liu D, Marcolla B, Montagnani L, Raschi A, Rouspard O, Varlagin A, Wohlfahrt G (2014) Global comparison of light use efficiency models for simulating terrestrial vegetation gross primary production based on the LaThuile database. *Agr Forest Meteorol* 192–193: 108–120. doi:10.1016/j.agrformet.2014.03.007